International Journal of Research
Available at https://edupediapublications.org/journals
e-ISSN: 2348-6848
p-ISSN: 2348-795X
Volume 04 Issue 09
August 2017

Experimental Study of Electronic Transporte in TiO_2/Si Junctions

Dr. Radhyah Mahdi Shaker Jarrah
University of Kufa/ Faculty of Science/ Department of Physics
:

Abstract

In this work, a heterojunction TiO2 on Si base has been made by use the D.C magnetron sputtering method with Ti target and oxygen plasma. The film was deposited on Si wafer and then undergone to the annealing process at various annealing temperatures were employed to assess film properties. The capacitance with reverse bias has been measured as a function of bias voltage at frequency 10 kHz, and these measurements have indicated the width of the depletion layer (W) surges with increasing of annealing temperature. The current–voltage characteristic
It turned out through the current–voltage graph of TiO2/Si heterojunction the forward current at dark changes with change of applied voltage, in demeanor concordant with recombination-tunneling model.
The results have shown that the dark current rises with growth of Ta. Also under illumination condition its clear to show there is a positive correlation relationship between the photocurrent and Ta.

Keywords : magnetron sputtering, annealing , heterojunction, depletion layer, photocurrent, tunneling current .

1- Introduction

Titanium dioxide (Titania, TiO2) material has wide applications in optoelectronic fields due to their characterizes and properties. TiO_2 is one of the of transition metal oxides, there are three common polymorphs types for this material, anatase (tetragonal), and brookite (orthorhombic) and : rutile (tetragonal)[1].

Currently, it employ to use as an electrode in electrochemical systems, particularly for gas detection devices [1-5]. The molecular structure of Titanium dioxide (TiO_2) provides advantageous properties, for instance the high value of the dielectric constant, chemical stability, mechanical rigidity, besides the perfect insulating properties. The optical transmittance and high refractive index within the extend of the visible spectrum, for the Titanium dioxide made it a suitable material for using as protective coatings for very large-scale integrated circuits [6, 7].

The most common method to prepare TiO2 thin films is the reactive sputtering, in this technique offers the possibility to use , evaporation rates, pressures of reactive gases, and , and substrate temperatures to control and adjust the packing density of the films. The D.C. sputtering process involves electron ejecting from the cathode material and forced to move away from it, by exploiting appropriate magnetic field to make the electrons take circular orbits and stay near the target surface, that give rise to growth high flux of electrons and creates high density plasma, this plasma is utilized to pluck out target atoms and then directed towards the substrate [8-10].

Heterojunction is a semiconductor interface formed between two different types of semiconductors. These two semiconductors are assumed possess different values of energy gap (E_g), permittivity (ε_s), work functions (Φ_m), and electron affinities (χ) as well as a difference in lattice constant. Heterojunction has been widely studied, and there are many essential applications have exploited this formation [11, 12]

2- Experimental prate.

2. 1 Magnetron Sputtering:

d.c magnetron sputtering a circular magnetron with 10 cm diameter and 400 Gausses was used. The discharge characteristics have been controlled using variable d.c supply (5kVand 500 mA) Pure Ti (99.99%) (LB) with a diameter of 10 cm and 0.4 cm thickness was used as a sputtering target;

The first step before the starting of the deposition process, it was the evacuation of the growth chamber, then Ar (99.99%) gas was introduced into the chamber as working gas. The chamber total pressure was fixed at 0.6 Pa during the whole deposition. A direct voltage (power was maintained at 100W) was applied and O_2 (99.99%) gas was introduced into the chamber as effective gas.

2.2 X-Ray Diffraction spectra

The structural properties were studied using X-ray diffraction measurements have been done and identified according to the JCPDS cards (Brookite, Anatase and Rutile [13-15]. X-ray diffractmeter system, Miniflex(600), with capper K_α radiation of wavelength λ= 1.5408A° was used. The X-ray diffraction of a crystal can be formulated by means of Bragg's law :

$$2d\ Sin\theta = n\lambda \quad \ldots\ldots\ldots\ldots\ldots\ldots\ldots\ldots(1)$$

where d is the d-spacing, perpendicular distance between pairs of adjacent planes in the crystal.
The peaks of thin films was used to determine the average grain size using Scherrer's equation [16]:

$$D = \frac{0.9\lambda}{\beta\ Cos\theta} \quad \ldots\ldots\ldots\ldots\ldots\ldots\ldots\ldots (2)$$

Where D is the average grain size (nm), λ is the X-ray wavelength (1.5408 Å), β is the full-width at half-maximum (FWHM) intensity (in radians).

2.3 The Electrical Measurement of TiO_2 /Si Heterojunction

The capacitance measurements of the heterojunction as a function of the reverse bias voltage in the range 0.0-1.0 V were performed in dark using LCR meter model HP-R2CC 4274A.The test of the frequency was set at 10 kHz. The potential energy barrier at the junction can be calculated by using small-signal capacitance–voltage (*C*–V) graphs. it was found that the capacitance decreases with an rises in the reverse bias, so it is negative linear correlation between the square of the capacitor value and reverse potential difference, the built – in junction potential can obtained from the voltage axis intercept at C equal zero.Theoretically, the C–V characteristic is described by the conventional heterojunction relation: [17, 18]

$$C^2 = \frac{qN_D N_A \varepsilon_1 \varepsilon_2}{2(N_A\varepsilon_1 + N_D\varepsilon_2)} \frac{1}{(V_{bi} - V\ )} \quad \ldots\ldots\ldots\ldots (3)$$

Here, N_D and N_A is the donor density in n-TiO_2, the acceptor density in p-Si, ε_1 and ε_2 are the dielectric constants of n-TiO_2 and p-Si, respectively, V_{bi} is the built – in potential, and V is the applied voltage. The slope of this line gives the impurity concentration of the substrate (N_A).
The width of the depletion region can be calculated by: [19,20]

$$W = \varepsilon_s A_j / C_o \quad \ldots\ldots\ldots\ldots\ldots\ldots (4)$$

where C_o is the capacitance at zero biasing voltage, Aj is the effective area of the junction and ε_s is the permittivity of semiconductor calculated from the equation:

$$\varepsilon_s = (\varepsilon_1 \varepsilon_2) / (\varepsilon_1 + \varepsilon_2) \quad \ldots\ldots\ldots\ldots\ldots\ldots\ldots\ldots (5)$$

where ε_1 and ε_2 is the semiconductor permittivity of the two semiconductor materials.

The dark current as a function of forward and reverse bias voltage in the range (0.0-2.0 Volt) and (–2.0-0.0 Volt) respectively, for all prepared TiO_2 /Si junction with various annealing temperatures were carried out using keithley digital electrometer

616 and d.c power supply. The barrier height (φ_B) and ideality factors (β) are extracted by using the following equations [21].

$$I_s = AA^* T^2 e^{-q\phi_B / kt} \quad \ldots\ldots\ldots\ldots\ldots\ldots (6)$$

$$I = I_s (e^{qV/\beta kT} - 1) \quad \ldots\ldots\ldots\ldots\ldots\ldots (7)$$

where A is the cross-sectional area, A* is Richardson constant ,I_s is the saturation current and β is the ideality factor having a value between 1and 2.

The current is due to tunnelling that dominates across the junction and it could be represented by the expression: [22]

$$I = I_o \exp(\gamma v) \ldots\ldots\ldots\ldots\ldots\ldots\ldots\ldots\ldots\ldots\ldots\ldots (8)$$

From the plot of the forward current (I_f) versus applied forward bias voltage (V_f),

3- Results and discussion

X- Ray Diffraction was used to study the crystal structure of TiO_2 thin films, with different annealing temperature.

Fig (1) shows the TiO_2 thin films deposited on glass substrate for as deposited and annealing for different temperature 373K,473K and 573K for two hour in air. The first structure (as deposited) have peaks A(112), B(112) R(210), B(032) ,B(213), B(431) and A(224) at angles (2θ=38.6°), (2θ=39.9°), (2θ=44.7°), (2θ=46.3°), (2θ=64.9°), (2θ=78.7°) and (2θ=82.4°) respectively.

The XRD spectra of the TiO_2 thin film annealed at Ta=473K show the same result, and grown at Ta=573K show same result but the peak B (032) at angle (2θ=46.3°) was vanish. Indicating that the crystallinity of the films depends on the annealing temperature. No significant sign of structural transformation was observed in the X-ray diffraction patterns after annealing temperature to 573K.

The annealing treatment has affected both the full at half maximum (FWHM) intensities, and the peak position of XRD by which the peaks height increases while the peak width decreases with increasing the annealing temperature. The FWHM values are related to the grain size of the film. The smaller the FWHM lead to larger grain size and the better of crystal quality of the whole film. By increasing the annealing temperature, the grain size of film was increased as shown in Table (1). The peak of A(112) was dominated for all XRD samples. The average grain size was 26nm in (as deposited) thin film and increase to 27.7nm and 28.8nm after annealing from 673K to 773K respectively.

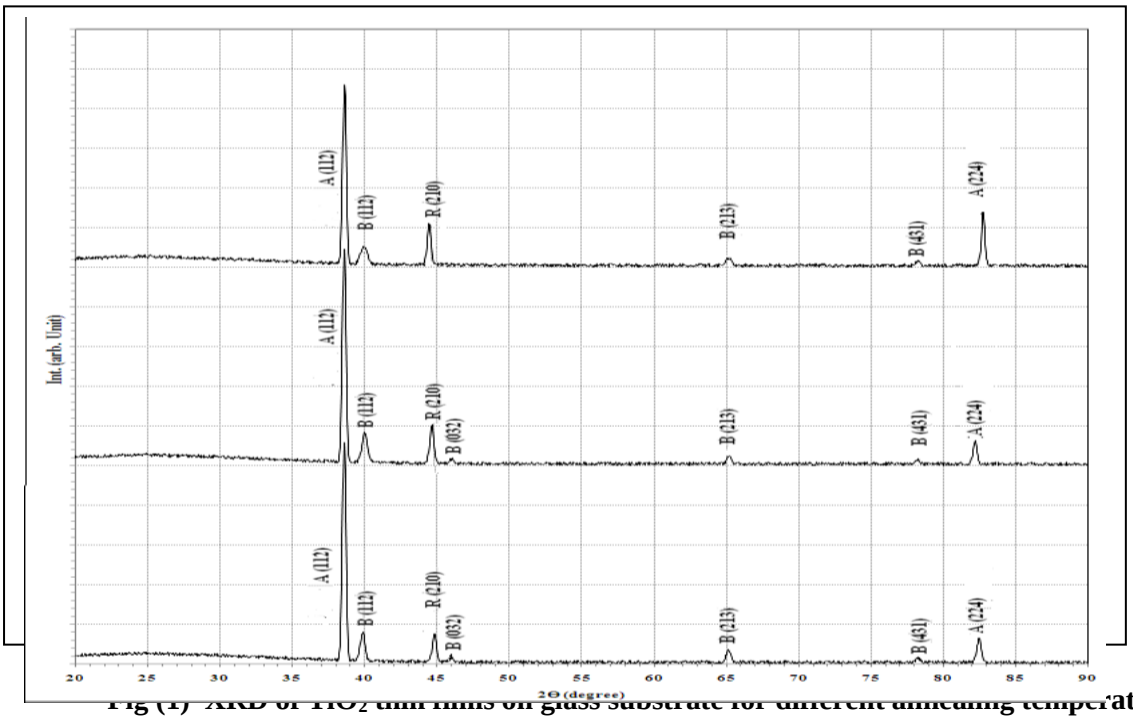

Fig (1) XRD of TiO_2 thin films on glass substrate for different annealing temperature.

Table (1) The experiment tal and stander

peaks [13] appear at XRD patterns at deferent annealing temperature.

T_a (K)	2θ(degree) (Exp.)	d_{hkl} (Å) (Exp.)	Grain size (nm)	d_{hkl} (std.) (Å)	Phase	(hkl)
373	38.606	2.330	27.51	2.332	Anatase	(112)
	39.961	2.254	22.48	2.254	Brookite	(112)
	44.748	2.024	28.08	2.054	Rutile	(210)
	46.374	1.956	24.69	1.433	Brookite	(032)
	64.981	1.434	20.0	1.434	Brookite	(213)
	78.710	1.215	30.22	1.220	Brookite	(431)
	82.413	1.169	29.91	1.166	Anatase	(224)
473	38.587	2.331	28.06	2.332	Anatase	(112)
	39.974	2.254	24.15	2.254	Brookite	(112)
	44.690	2.026	27.71	2.054	Rutile	(210)
	46.077	1.968	26.98	1.433	Brookite	(032)
	65.218	1.429	28.67	1.434	Brookite	(213)
	78.256	1.221	30.75	1.220	Brookite	(431)
	82.232	1.171	29.87	1.166	Anatase	(224)
573	38.587	2.331	29.02	2.332	Anatase	(112)
	39.881	2.259	21.13	2.254	Brookite	(112)
	44.412	2.038	28.6	2.054	Rutile	(210)
	65.125	1.431	31.42	1.434	Brookite	(213)
	78.256	1.221	32.0	1.220	Brookite	(431)

	82.787	1.165	31.15	1.166	Anatase	(224)

The electrical properties of these structures are analyzed from capacitance-voltage (C-V) and current-voltage (I-V) characteristics. The results demonstrated that all the samples show strong rectifying behavior.

The photovoltage extremely depends on the built- in potential of heterojunction, therefore, C-V characteristics were performed in order to examine the built-in potential of the samples. The changing of capacitance as a function of reverse bias voltage for TiO_2 /Si heterojunction with different annealing temperature T_a shown in figure (2). It is clear that the capacitance decreases with the raise of T_a. this behavior is attributed to the increasing in the depletion region width and also due to the decrease in the surface states [23].

The growth of the width of depletion layer with creasing of the Ta could be due to the decreasing in the carrier concentration which leads to a decrease of the capacitance as given in table (2). Figure (3) shows the inverse capacitance square is plotted against applied reverse bias voltage for TiO_2 /Si junction at different T_a. From the same figure, we have deduced the carrier's concentration of the abrupt TiO_2 /Si heterojunction at different T_a from the slope of the straight line. Table (2) exhibits that these values which decrease with increasing T_a.

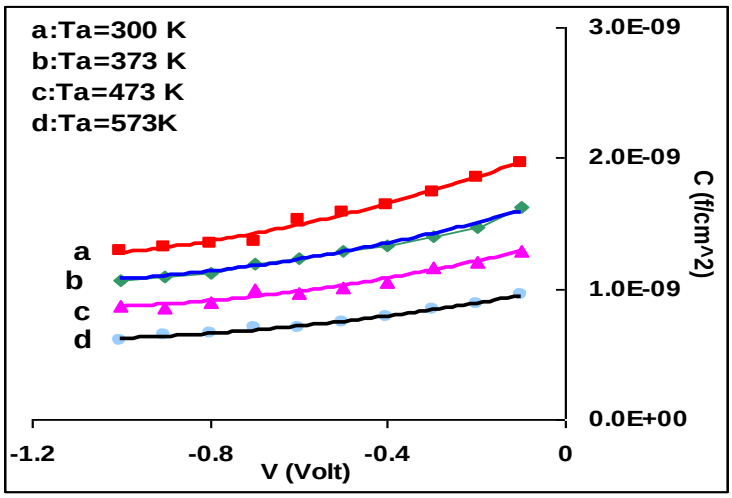

Fig.(2) Variation of capacitance as a function of reverse bias voltage for TiO_2 /Si junction at different T_a.

Figure (4) shows the I-V characteristics of TiO_2 /Si heterojunction with different value of Ta. As shown, the reverse currents are very weak and the forward currents increase sharply with the bias voltage. This testifies that the samples show apparently rectifying behavior.

The main source of the forward dark current is the flow of majority carriers, which are injected by the applied voltage and give rise to decrease of the width of the depletion layer. When the majority and minority carrier concentration is higher than the intrinsic carrier concentration ($n^2_i < np$) may cause togenerate of the recombination current at lower voltage region. This is because the excitation of electrons from the valence band (V.B.) to the conduction band (C.B.) will recombine them with the holes which are found at the V.B, and this is observed by the little increase in recombination current at low voltage region, while the tunneling current occurs at the high voltage region. The reverse bias current also contains two regions figure (5). In the first region of low voltages, the current slightly increases with increasing of the applied voltage, and the generation current dominates, while in the second high voltage region, the diffusion current dominates [20,21].

We also observed that the current increases with increasing of T_a because the increasing of temperatures will cause rearrangement of the interface atoms and reduce the dangling bond which leads to the improvement of the junction characteristics [24].

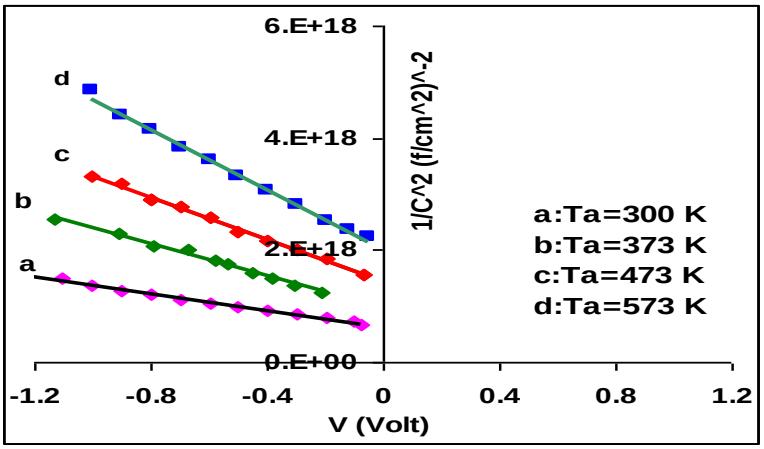

Fig. (3) the variation of $1/C^2$ as a function of reverse bias voltage for TiO_2 /Si heterojunction at different T_a.

Table (2) Values of W, N_D, and V_{bi}, for TiO_2/Si hetrojunection at different T_a.

T_a (K)	V_{bi} (Volt)	C_o (nf/cm^2)	W (nm)	N_D (cm^{-3})
300	0.761	5.91	324	4.14×10^{15}
373	0.793	5.72	382	$2.11\text{x}10^{15}$
473	0.825	5.55	412	$8.4\ 6\text{x}10^{14}$
573	0.852	5.11	465	$4.73\text{x}10^{14}$

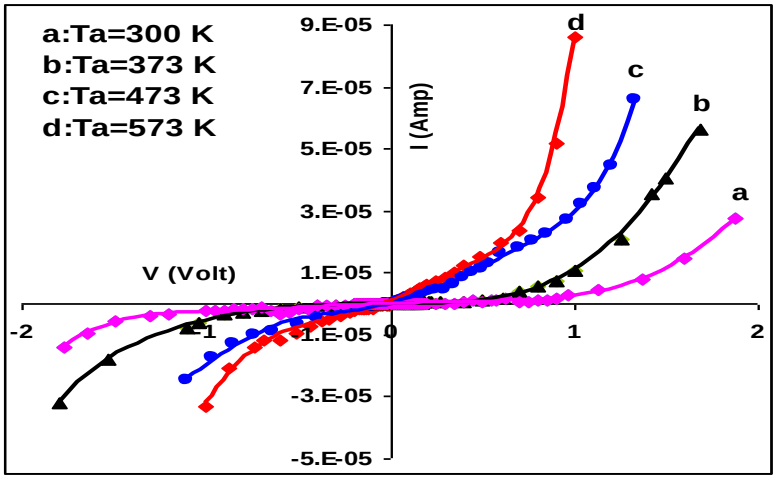

Fig. (3) I-V characteristics under dark for TiO_2/Si heterojunction at forward and reverse bias voltage at different T_a.

Figure (5) shows the semi–log relation between dark forward current density and bias voltage (0-2.5) volt for TiO_2/Si junctions at different T_a. The mechanism of the forward current coincides with the recombination tunneling mechanism [25], its clear from this figure that the saturation current decreases with T_a.

The current transport across the semiconductors interface dependent on temperature, thus, the electrons at low temperature would be able to cross only the lower barriers and therefore current transport will be dominated by current passing through the lower barrier. With increasing temperature, more and more electrons would acquire significant energy to cross higher barrier.

The barrier height (Φ_b) and ideality factor, seems that they have increasing with T_a as shown in table (3). These increases may be associated with the increase of the available charge carriers to be transported across the barrier for Fermi level equalization.

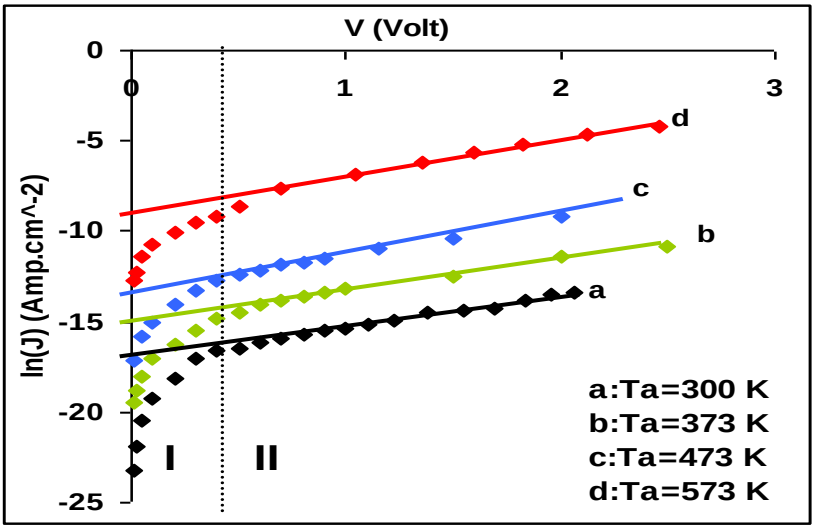

Fig. (5) ln (J) versus *V* for forward bias of dark of the fabricated TiO_2/ Si heterojunction at different Ta.

Table (3) Ideality ,tunneling factor the barrier height and saturation current values for TiO2/Si heterojunction at different Ta.

T_a (K)	Ideality Factor(β)	Tunneling Factor $(\gamma)(V)^{-1}$	Φ_b eV	I_s μ Amp
300	3.25	3.9 2	0.695	2.1
373	2. 44	3.59	0.721	1. 8
473	1. 80	3.17	0.763	1.1
573	1.23	2.83	0.789	0.4

Conclusions

The XRD analysis showed that TiO_2 thin films was polycrystalline and have three phases mixture (Rutile, Anatase and Brookite).

This work has two main measurement, the C-V and I-V for the TiO_2 Heterojunction, according to the results of first measurement (C-V) the capacitance decreases with the both increasing of the reverse bias voltage and Ta, also the width of the depletion layer increases with increasing of Ta.

the second measurement (I-V) indicate there were rectifying behavior, and the dark current increases slightly with increasing of Ta. Also easy to realized the barrier height (Φ_b) increase with Ta.

Reference

[1] C. Garzella, E. Comini, E. Tempesti, C. Frigeri, and G. Sberveglieri, [*TiO_2 thin films by a novel sol-gel processing for gas sensor applications*], Sensors and Actuators B: Chemical 68, (2000) ,p. 189-196.

[2] D. T. Cromer and K. Herrington[The structures of anatase and rutile] Journal of the American Chemical Society 77,(1955),p. 4708–4709.

[3] J. Nowotny, C.C. Sorrell, L.R. Sheppard, and T. Bak, [*Solar-hydrogen: Environmentally safe fuel for the future*] Int. J. Hydrogen Energy, 30, (2005), p. 521-544.

[4] L. Francioso, D.S. Presicce, P. Siciliano, and A. Ficarella, [*Combustion conditions discrimination properties of Pt-doped TiO_2 thin film oxygen sensor*] Sensors and Actuators B: Chemical 123, (2007) , p.516-521.

[5] Y. Shimizu, N. Kuwano, T. Hyodo, and M. Egashira, [High H_2 sensing performance of anodically oxidized TiO_2 film contacted with Pd] Sensors and Actuators B: Chemical 83, (2002), p. 195-201.

[6] D. Bersani, P.P. Lottici, X.Z. Ding, [Phonon Confinement effects in the Raman Scattering by TiO_2 nanocrystals],Applied physics Litters. 72, (1998), p. 73-76.

[7] G.S.Brady, Materials Handbook, 10th edition, McGraw-Hill, NewYork,1971, p. 815.

[8] J. Musil, P. Baroch, J. Vlcek, K .H. Nam, and J. G. Ham [Reactive magnetron sputtering of thin films] ,Thin Solid Films 475,(2005), p. 208-218.

[9] S. Berg and T. Nyberg [Fundamental understanding and modeling of reactive sputtering processes] ,Thin Solid Films 476,(2005) ,p. 215-230.

[10] D. Gttler, B. Grtzscchel and W. Mller, [Mechanisms of Target Poisoning *During* Magntron Sputtering] ,Applied Physics Litters 85,(2004), p.6134-6146.

[11] S. M. Sze, Kwok K. Ng., Handbook[Physics of Semiconductor Devices], .Third Edition, John Wiley and Sons, JNC. Publication, (2006).

[12] J. Loferski, Handbook,[Optimization of II–VI based heterojunctions], Solid-State Electron, V. 30, N.11,(1987) ,p. 1205.

[13] JCPDS Data Base, Card No. 29-1360

[14] JCPDS Data Base, Card No. 21-1272

[15] JCPDS Data Base, Card No. 21-1276

[16] Y.Arai, R. J Akers and C. R. G. Treasure[*Chemistry of powder production*] 1st English language ed.; Chapman & Hall: London, (**1996**)281.

[17] B.Sharma and R. Purohit, Handbook [Semiconductor Heterojunction], First edition, Vol. 5,(1974).

[18] B.L.Sharma, R.K.Purohit and S.N.Mukerjee,[Detectivity calculations for photo voltaic heterojunction detectors], Infrared Physics,vol.10,(1970) p. 225- 231.

[19] M.J.Adams and A.Nussbaum,[Theory of abrupt heterojunctions in equilibrium], Solid State Electron , vol.22 ,(1997) ,p. 783-791.

[20] Morgan and K.Board, Handbook [An Introduction to Semiconductors Micro- technology], John weley and Sons,Inc.Newyork,(1991).

[21] G. Zeidenbergs and R. Anderson, Handbook [Energy barriers and interface states at heterojunctions],Solid-State Electron, Vol.10, (1967), p.113.
[22] S. Al-Heniti1, R. I. Badran2, et al., [Temperature Dependant Structural and Electrical Properties of ZnO Nanowire Networks], Journal of Nanoscience and Nanotechnology Vol. 11, (2011), p. 1–7.
[23] H.M. Zeyada, M.M. El-Nahass, et a, [Study of Structure and Electro-Optical Characteristics of Indium Tin Oxide Thin Films] J. Appl. Phys. 49, (2010),p. 10301,
[24] D. Song, D. H.Neuhaus, J. Xia, A.G. Aberle, Handbook [Thin Solid Films] 422,(2002), p. 180 .
[25] M.Burgelman, P.Nollet and S.Degrave, Handbook [Applied Physics], A,69,149, (1999), p. 423 -434